Letter

Unusual stability of protein molecules in the presence of multivalent counterions

Sugam Kumar,[1] Debasish Saha,[1] Debes Ray,[1] Sohrab Abbas,[1] and Vinod K. Aswal[1,2,*]
[1]*Solid State Physics Division, Bhabha Atomic Research Centre, Mumbai 400 085, India*
[2]*Homi Bhabha National Institute, Mumbai 400 094, India*

(Received 31 December 2020; revised 25 May 2021; accepted 8 July 2021; published 29 July 2021)

Proteins are known to undergo denaturation and form different phases with varying physicochemical parameters. We report unusual stability of bovine serum albumin protein against commonly used denaturants (temperature and surfactant) in the charged reversal reentrant phase, caused by the multivalent counterions. Unlike monovalent counterions, which promote the denaturants' induced protein unfolding, the unfolding is restricted in the presence of multivalent ions. The observations are beyond the scope of general understanding of protein unfolding and are believed to be governed by ion-ion correlations driven strong condensation of the multivalent ions.

DOI: 10.1103/PhysRevE.104.L012603

Proteins are one of the most abundant and versatile biomolecules which play a crucial role in almost all essential processes taking place in organisms. The functioning of the proteins is usually directed by their three-dimensional folded structure, which is known to be perturbed by specific physicochemical conditions (e.g., temperature, pressure, etc.) and/or presence of certain additives (urea, surfactant, etc.) [1–3]. Such perturbations lead to the unfolding (denaturation) of the protein which may be unwanted in some cases or may be deliberate many times as required for various industrial as well as scientific applications [4]. Nevertheless, understanding and tuning the protein folding and unfolding has always been of great research interest to establish the control over its functioning and regulate biological activity.

The denaturation process based on the denaturant follows a specific mechanism [2,3,5–8]. For example, the presence of surfactants unfolds the protein polypeptide chain by binding itself with the hydrophobic patches of the chain where electrostatic as well as hydrophobic interactions both play an important role [6,7,9]. On the other hand, an increase in the temperature leads to the disruption of the hydrogen as well as disulfide bonds and finally exposing the hydrophobic groups which thereby gives rise to hydrophobic attraction-driven gelation of the proteins at significantly elevated temperatures [3,7,10]. The addition of urea forms hydrogen bonds with the peptide backbone and breaks some of the hydrogen bonds of the nearby water molecules leading to the denaturation of the protein molecules [8]. Overall, it is the interplay of different inter- and intramolecular interactions that decides if the protein will remain in the folded or unfolded structure under specific circumstances [3,5,11].

The interactions in globular protein solutions may be predicted by the well-established colloidal theories (e.g., Derjaguin-Landau-Verwey-Overbeek or Debye-Hückel theory) as these proteins are usually considered as colloids [12,13]. However, these theories are known to have several limitations [14,15]. Moreover, different factors such as nonuniform charge distribution, complicated structural bonding, intrinsic flexibility, and the presence of nonclassical interactions give rise to intriguing behavior of the protein molecules [13–17]. It has been shown that even the presence of different valent counterions exhibits significant differences in the protein phase behavior [12,18–20]. For instance, the addition of monovalent counterions in the biological salt concentration limits leads to a nonmonotonic behavior of the interaction potential [17]. Moreover, the presence of multivalent salts gives rise to an interesting reentrant phase behavior in proteins, where the protein solution transforms from one phase (stable individual protein) to two phase (protein aggregation) and then back to one phase (individual protein) as a function of multivalent counterion concentration [12,18,21]. The significantly prevailing ion-ion correlations in multivalent counterions cause excessive condensation of the ions on the proteins, which in turn reverse the charge of proteins, giving rise to the reentrant phase behavior [18]. The multivalent ions have the potential to anomalously alter the double layer around the protein molecules (colloids in general) and hence electrostatic interaction between themselves and with other molecules present, leading to the emergence of several counterintuitive phenomena (e.g., overcharging, like-charge attraction, etc.) and reentrant behavior in physical properties [18–24]. In fact, the multivalent ions are reported to be providing the unexpectedly enhanced stability to the uniformly charged nanoparticles against the monovalent counterions [25]. Considering the importance of the electrostatic interaction in the protein denaturation, the multivalent ions are expected to tune the protein folding and unfolding.

In this paper, we report the ability of the multivalent ions to restrict the unfolding of the protein as otherwise easily caused by the well-known denaturants (heat and surfactant). Unlike monovalent ions, which promote the protein unfolding as driven by increase in the temperature and addition of surfactant, the protein in the presence of multivalent counterions

*vkaswal@barc.gov.in

shows resistance against such unfolding. Small-angle neutrons scattering (SANS) and dynamic light scattering (DLS) have been used to understand the propensity of the unfolding (if any) induced in the proteins. Bovine serum albumin (BSA) has been used as a model system while the salts $AlCl_3$ (trivalent Al^{3+}) and $ZrCl_4$ (tetravalent Zr^{4+}) for providing multivalent counterions. It should be mentioned here that such acidic salts usually lead to partial denaturation of the protein. However, despite metal salt-induced slight disruption in the protein structure, our findings show that the multivalent salt restricts any further unfolding of the protein which is otherwise easily driven by denaturing agents. The BSA (5 wt. %) solutions were prepared without and with multivalent salts and in the absence and presence of denaturants, in acetate buffer at pH 7, where BSA carries an effective negative charge. No further attempts were made to maintain the pH of the solution. However, changes in the pH on addition of $ZrCl_4$ are monitored and provided in Supplemental Material (Fig. S1) [26], as the strong hydrolysis of $ZrCl_4$ causes reduction of the solution pH. The decrease in the pH value is substantially less in the presence of BSA, compared to that of the pristine buffer. At 30 mM $ZrCl_4$, the pH of 5 wt. % BSA solution is observed to be ∼4, which is higher than that of the pure buffer solution (∼2), in the presence of the same amount of $ZrCl_4$.

Further details on the sample preparation and experiments can be seen in Supplemental Material [26]. First, the phase behavior (Figs. S2 and S3 in Supplemental Material [26]) of the protein solutions in the presence of salts is examined and found to exhibit reentrant behavior, as described above as well as in Supplemental Material [12,18]. The multivalent salt concentrations are then chosen in the reentrant regime, where effective counterions condensation on the protein molecules results in charge reversal of proteins (cationic BSA), thereby restabilizing the system [12,18]. The zeta potential measurement of BSA protein with $ZrCl_4$ also supports the charge alteration (Fig. S4 in Supplemental Material [26]). In this case at higher salt concentrations, the pH of the solution can be below the isoelectric point, which in combination of the multivalent counterions condensation can give rise to high reversed charge to the proteins [27]. However, the behavior of the BSA in the presence of $ZrCl_4$ is completely different than that of the same system (5 wt. % BSA) prepared in the buffer of the equivalent pH without $ZrCl_4$. It has been shown that the observations are neither solely directed by the change in the pH nor in the ionic strength, and the presence of multivalent Zr^{4+} plays an important role, as discussed later.

Figure 1 depicts the temperature-driven denaturation and finally gelation of the BSA (5 wt. %) protein in pristine as well as in salt solution [monovalent (NaCl, 500 mM) and tetravalent ($ZrCl_4$, 30 mM)]. The physical states of the samples at 85 °C are presented in Fig. 1(a). In the absence of any salt, the system transforms into a translucent gel, having minuscule flowing characteristic, whereas the addition of the monovalent salt promotes the gelation and the system forms a relatively rigid (nonflowing) and white gel. Unlike both of these cases, in the presence of $ZrCl_4$ the system does not transform into the gel state, but rather maintains its liquidlike flowing character. The sample behavior in the presence of NaCl is in accordance with the classical colloidal theories which assume the reduction of the Coulomb barrier due to increased ionic strength,

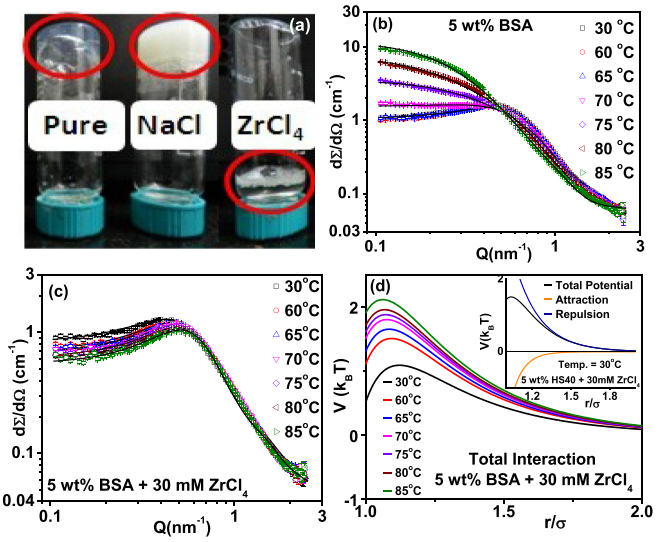

FIG. 1. (a) Physical state of the 5 wt. % BSA solution in the absence of any salt and in the presence of 0.5 M NaCl and 30 mM $ZrCl_4$ salts at 85 °C. SANS data of the (b) 5 wt. % BSA and (c) 5 wt. % BSA+30 mM $ZrCl_4$ samples with varying temperature. (d) Total interaction potentials of 5 wt. % BSA+30 mM $ZrCl_4$ with increasing temperature. The inset shows the total potential along with the attractive and repulsive components for the same system at 30 °C.

responsible for the accelerated gelation. On the other hand, the observation for tetravalent salt is counterintuitive, as Zr^{4+} ions are expected to be more assistive for temperature-stimulated protein gelation, as per Hofmeister Series. The behavior of pure 5 wt. % BSA (no salts) solution prepared in the pH 4 transforms into the translucent gel on keeping it at around 70 °C for nearly 2 h (Figs. S5 and S6 in Supplemental Material [26]). This suggests that the stability of the BSA solution against temperature is not due to reduction in the pH. In fact, it has been shown that the decrease in pH can even result in gelation at temperatures as low as 37 °C at higher protein concentrations [28]. Moreover, in the presence of 300 mM NaCl (equivalent ionic strength to 30 mM $ZrCl_4$), the 5 wt. % BSA solution (pH ∼2, 3, 4) also transformed into gel at 70 °C. It may be noted that the macromolecular crowding which stabilizes proteins against unfolding can be expected at such high protein concentration (5 wt. %). However, in the present study it was not possible to achieve the protein gelation at sufficiently low concentrations (e.g., 1 wt. %) with the used $ZrCl_4$ concentrations. Moreover, it has been shown that it is easier to achieve the gelation at higher BSA concentrations, because of the higher possibility of the cross linking [29,30].

To understand such peculiar behavior at the microscopic level, we have carried out SANS measurements. The SANS data of 5 wt. % BSA protein in pristine and in the presence of tetravalent counterions with varying temperature are shown in Figs. 1(b) and 1(c), respectively. In SANS, one measures the coherent differential scattering cross section per unit volume $[d\Sigma/d\Omega(Q)]$, as a function of scattering vector $[Q = 4\pi \sin(\theta/2)/\lambda$; neutron wavelength λ and scattering angle $\theta]$ and expressed as $\frac{d\Sigma}{d\Omega}(Q) = \varphi V(\rho_p - \rho_s)^2 P(Q) S(Q) + B$, where φ and V are the volume fraction and volume of the individual scatterer, respectively [31]. ρ_p and ρ_s represent the

scattering length densities of scatterer and solvent, respectively. $P(Q)$ is the intraparticle structure factor (square of the particle form factor) which provides the geometrical parameters of the particles. $S(Q)$ denotes the interparticle structure factor which is governed by the interparticle interactions. B denotes the incoherent background. Details of the data correction and analysis are provided in Supplemental Material.

The SANS data [Fig. 1(b)] of the pure 5 wt. % BSA at 30 °C show a correlation peak, which is indicative of the presence of interacting scatterers and usually appears at $Q{\sim}2\pi/d$ (where d is the interparticle separation). The concentration of the protein solution for SANS measurements is taken as 5 wt. % to clearly observe this peak, which enables the quantification of the modifications in the interactions between proteins, on addition of different salts (additives) and physiochemical conditions [32,33].

The data of the pure BSA (without any additive) have been fitted using a form factor of oblate ellipsoidal shape with an interparticle structure factor as calculated for a two-Yukawa (2Y) potential, which may be written as $\frac{V_{2Y}(r)}{k_BT} = +K_1\frac{\exp[-Z_1(r/\sigma-1)]}{r/\sigma} - K_2\frac{\exp[-Z_2(r/\sigma-1)]}{r/\sigma}$, where interparticle distance is represented by r and σ is equivalent hard-sphere diameter of the protein [34,35]. The first term represents the interparticle repulsion between the proteins, while the second one is to account for the interparticle attraction. The potential contains four unknown parameters K_i ($i = 1, 2$) and Z_i which represent magnitude and range ($1/Z$) of the respective part of the potential. For pure BSA, the repulsion is accounted for by screened Coulomb interaction while the attraction is considered by parameters equivalent to the van der Waals interaction. The protein molecules are found to have a semimajor ($b = c$) axis 4.2 nm, semiminor axis (a) 1.4 nm (Table ST1, Figs. S7, S8, and S9 in Supplemental Material [26]) [12]. The BSA conformation is found to be slightly extended in the presence of $ZrCl_4$, with semimajor ($b = c$) axis 5.0 nm, and semiminor axis (a) 1.4 nm (Fig. S9 in Supplemental Material [26]) [36]. We have also calculated the values of the radius of gyration (R_g), maximum size of the object (D_{max}), molecular weight (M_W), and pair distance distribution function [$P(r)$] for the samples 1 wt. % BSA and 1 wt. % BSA+30 mM $ZrCl_4$ (Fig. S10 and Table ST2 in Supplemental Material [26]). In the case of the pure BSA, the M_W is found to be quite close to that of the monomer and the data of 1 wt. % BSA could be well fitted with the proper crystal structure of the BSA monomer obtained from the Protein Data Bank (PDB file code 4F5T). However, the M_W as well as R_g of 1 wt. % BSA+30 mM $ZrCl_4$ are found to be higher than those of the pure BSA, suggesting the possibility of the presence of mixture of monomers and dimers in the solution. It may be noted that the data of 1 wt. % BSA+30 mM $ZrCl_4$ could neither be fitted with the crystal structure of monomer nor dimer alone. However, the $P(r)$ curve does not show the presence of any secondary peak, indicating the presence of the dimers (if any) in sufficiently low concentration, not able to contribute significantly in the scattering intensity. Therefore, we finally analyzed the data based on the existence of the extended protein conformation at low pH. It will further be interesting to examine the possibility of tuning of the monomers to dimers ratio using multivalent salts.

On increasing the temperature, the SANS data show almost no change in the scattering profile up to almost 65 °C but a sharp and linear increase in the scattering intensity for temperatures above 70 °C, suggesting the temperature-driven denaturation of the protein which finally results into a translucent gel at about 80 °C. The data in this case have been analyzed by considering the evolution of the strong attraction between the unfolded protein molecules (Table ST3 in Supplemental Material [26]) [12,35].

The SANS data of the 5 wt. % BSA protein solution in the presence of monovalent salt (500 mM NaCl) are also presented in Fig. S11 in Supplemental Material [26]. The addition of 0.5 M NaCl in the BSA does not alter any structural parameters (Table ST1 and ST4 in Supplemental Material [26]); however, the correlation peak in the SANS data as observed in pure BSA solution at 30 °C disappears, as expected due to the enhanced ionic strength. On increasing temperature, the data in this case also show an increase in the scattering intensity, but more prominent than that observed for the pure BSA solution at a given temperature, confirming that monovalent salt assists the temperature-driven gelation of the protein by screening the charge-charge repulsion between the protein molecules. However, it has been reported that such screening of NaCl is less effective at sufficiently high protein concentrations ($\geqslant$200 mg/ml), due to strong steric interactions [29].

On the other hand, the SANS data of the 5 wt. % BSA+30 mM $ZrCl_4$ show similar scattering features irrespective of the temperature, without any signature of the attraction or aggregation. In fact, in the presence of $ZrCl_4$, the data show correlation peak despite the high ionic strength, suggesting the excessive condensation of the tetravalent counterions on the proteins, leading to the giant charge inversion, where the protein molecule carries the high reversed charge which is opposite in sign but more in magnitude compared to that in the pristine solution (without any multivalent ion) [37]. It is probably the strong hydration interactions originated from increased surface dipoles due to condensed Zr^{4+} ions, not allowing the exposure of the hydrophobic patches of the protein, and hence preventing the protein gelation.

The peak position [Fig. 1(c)] and scattering profile remain nearly the same with the rise in temperature suggesting that the protein molecules do not significantly change their shape. No changes in the SANS data, particularly in the high-Q range ($\sim$ 0.5 to 3 nm^{-1}), where the scattering is dominated by the form factor [$P(Q)$] of the individual protein molecules, suggests no further modifications in the protein structure on increasing temperature. This has been further confirmed by measuring the SANS data of the diluted samples (1 wt. % BSA), where the interparticle structure factor [$S(Q){\sim}1$] contributions can be neglected (Fig. S12 in Supplemental Material [26]) [38,39]. At this concentration also, no significant changes in the scattering data were observed on increasing the temperature. However, at 5 wt. % BSA concentration [Fig. 1(c)], the scattering at the low-Q region ($Q{\rightarrow}0$) decreases as the temperature increases, indicating that the interprotein interaction is rather becoming more repulsive at elevated temperatures, contradictory to the outcomes for the pristine BSA solution and in the presence of monovalent ions. The interaction between protein molecules has been

again modeled using the 2Y potential, keeping the attractive (corresponding to the van der Waals attraction) and structural parameters fixed. The parameters of attraction were kept fixed, as the addition of the salts is not anticipated to cause significant changes in the van der Waals attraction, whereas repulsive attraction is expected to undergo modifications, not only by the strong condensation of the multivalent salts but also by the changes in the physicochemical conditions (e.g., increase in temperature may lead to counterions dissociation or presence of similarly charged micelles may modulate the repulsive interaction). The total potentials for 5 wt. % BSA+30 mM $ZrCl_4$ as a function of temperature are shown in Fig. 1(d). A clear increase in the magnitude of the interprotein repulsion can be observed, possibly due to counterion (Cl^-) dissociation with increasing temperature. Recall that charge inversion of BSA at 30 mM $ZrCl_4$ concentration, Zr^{4+} ions are no more counterions, rather it is the Cl^- ions [12].

So far, it is demonstrated that tetravalent ions have modified the interprotein interactions and could restrict temperature-driven unfolding. We further examined the effect of the multivalent ions on the surfactant-induced protein unfolding to understand if these ions can also alter the intraprotein interactions, which are important for protein unfolding as caused by surfactant. The surfactants, particularly ionic surfactants [e.g., sodium dodecyl sulfate (SDS), dodecyltrimethyl ammonium bromide (DTAB), etc.) induced unfolding of the proteins, and related SANS data are well studied in the literature [5,6,9]. It is believed that the interaction of the surfactant with protein is primarily governed by an interplay of the electrostatic (between the charged head group and oppositely charged patches of the protein) as well as hydrophobic interactions (between hydrophobic patches on the protein and surfactant hydrophobic tails), where both of these interactions together perturb the intrachain bonding [5,6].

Figure 2 shows the SANS data of the 5 wt. % BSA with varying concentrations (C_D) of DTAB, without [Fig. 2(a)] and with $ZrCl_4$ [Fig. 2(b)]. In the absence of $ZrCl_4$, the correlation peak of BSA disappears on addition of surfactant; instead, the SANS data show a scattering buildup with linearity in the intermediate-Q range between the two Q cutoffs. These are the signatures of the formation of the bead-necklacelike structures where the surfactant micelles (beads) form around the hydrophobic patches of the unfolded polypeptide chain of protein. The data are analyzed using the random flight model, representing a beads-on-a-stringlike cluster. The model fitting provides the size of the micelles organized along the protein chain, the number (N) of micelles per cluster, and the separation (D) between the centers of two nearest micelles [40,41]. The fitted parameters (Table ST5 in Supplemental Material [26]) show that the unfolding of the protein is enhanced on increasing the surfactant concentration, as indicated by increasing D and decreasing N. Similar to the observation with temperature, the presence of monovalent salt encourages the protein unfolding by promoting the complexion of the protein and surfactants via suppression of the electrostatic repulsion between them [9].

However, in the presence of multivalent ions, the SANS data [Fig. 2(b)] do not show any signature of the bead-necklace structure formation; rather, the typical correlation

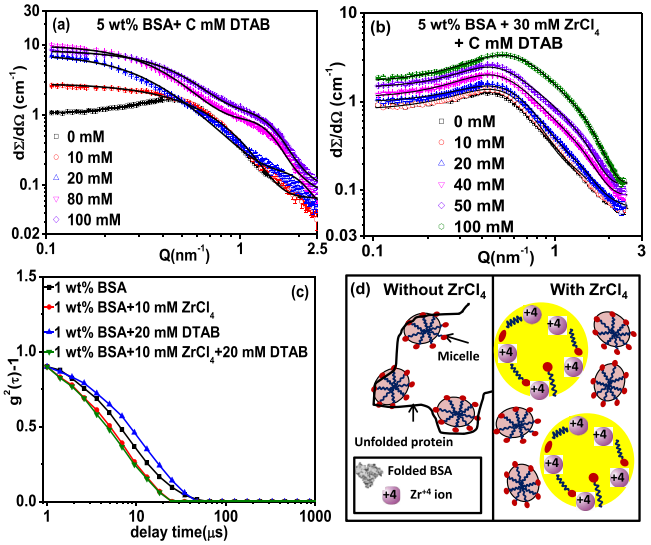

FIG. 2. SANS data of the 5 wt. % BSA protein with varying concentrations of the DTAB surfactant (a) in the absence of any salt (b) in the presence of 30 mM $ZrCl_4$. (c) Autocorrelation functions of 1 wt. % BSA with and without surfactant and $ZrCl_4$. (d) A scheme depicting possible mechanism through which condensation of $ZrCl_4$ prevents the protein unfolding which is otherwise easily carried out by surfactant.

peak corresponding to the interacting BSA molecules is observed. The correlation peak does not significantly shift; however, the scattering intensity increases with increasing surfactant concentration. Moreover, there is almost no significant change in the scattering profile observed for $C_D < 20$ mM. A buildup of scattering in the high-Q region with increasing surfactant concentration ($C_D \geqslant 20$ mM) is observed and is attributed to the free micelles in the system. The data in this case have been analyzed by considering the coexistence of BSA and micelles (Sec. S.4, Figs. S13 and S14, and Tables ST6 and ST7 in Supplemental Material [26]). However, the fraction of free micelles is relatively small, when compared with the pristine DTAB solutions, suggesting that some amount of surfactant as monomers attach to the BSA molecules in a noncooperative manner [Fig. 2(d)]. These monomers though bind to the oppositely charged patches of the protein, leading to the increase in the scattering contrast (intensity) but are not able to unfold the protein. We believe that the condensation of the Zr^{4+} ions does not allow many similarly charged monomers to form micelles along the protein chain and hence fully unfold it. It should be noted that in the absence of Zr^{4+} ions, even the similarly charged surfactants are also known to cause protein unfolding (e.g., BSA-SDS system) [9], suggesting that the condensation of the Zr^{4+} ions plays a crucial role in restricting the protein unfolding by surfactant. We further compared the SANS data of the 1 wt. % BSA+20 mM DTAB prepared at pH 2.4 with that of the same system in the presence of 30 mM $ZrCl_4$ (addition of $ZrCl_4$ reduces the pH of the solution from 7.0 to 2.4). The SANS data of the 1 wt. % BSA+20 mM DTAB (pH 2.4) show typical signatures of the bead-necklace kind of structure formation (Fig. S15 in Supplemental Material [26]). On the other hand, 1 wt. % BSA+20 mM DTAB+30 mM $ZrCl_4$ does not show any such

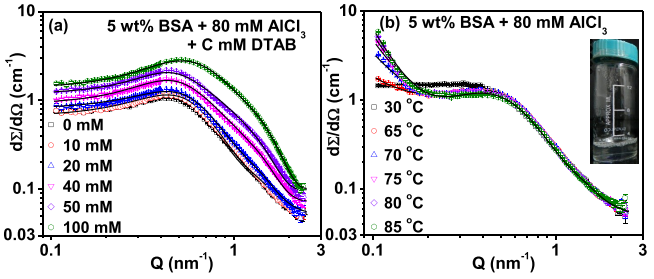

FIG. 3. SANS data of the 5 wt. % BSA +80 mM $AlCl_3$ with varying (a) DTAB concentration and (b) temperature.

conformation and the scattering profile can be treated by considering the contributions from two form factors (pristine BSA and DTAB micelles), again conforming that the observations cannot simply be explained based on reduction in pH.

The DLS measurements (details can be seen in Supplemental Material [26], Fig. S16) were also performed on the 1 wt. % BSA in the presence and absence of the DTAB/$ZrCl_4$ (20 mM/10 mM) and the measured autocorrelation functions (ACFs) are shown in Fig. 2(c). In the absence of $ZrCl_4$, the ACF of the BSA-DTAB system shifts towards longer relaxation times, compared with that of the pristine BSA (hydrodynamic size (D_h) $\sim$ 8 nm), indicating the formation of the larger structures ($D_h \sim 13$ nm) [9,41]. Opposite to this, in the presence of $ZrCl_4$, the ACFs of the of the mixed system (BSA-DTAB) move slightly towards the smaller relaxation times suggesting the decrease in the effective overall average size in the system ($D_h \sim 6$ nm). The faster decay in the BSA+$ZrCl_4$+DTAB system can be attributed to the evolution of the more repulsive interaction between BSA molecules, due to (i) condensation of the Zr^{4+} ions and (ii) the presence of similarly charged cationic DTAB micelles. No increase in the hydrodynamic size of the 1 wt. % BSA+10 mM $ZrCl_4$+20 mM DTAB system clearly demonstrates that DTAB in the presence of $ZrCl_4$ is not able to cause any significant unfolding of the protein, which could have led to the slower decay rate, as observed in the absence of $ZrCl_4$ [9].

The finding of suppression of the protein unfolding in the presence of $ZrCl_4$ is also confirmed by circular dichroism spectroscopy and the data of 5 wt. % BSA+30 mM DTAB sample with and without $ZrCl_4$ (diluted 200 times) are presented in Fig. S17 of Supplemental Material [26]. There is no additional unfolding, observed on addition of DTAB. It should also be mentioned here that metallic ions like Zr^{4+} may cause slight disruption in the protein structure; however, despite that, our observations suggest that the multivalent salt are able to prevent any further unfolding of the protein which is easily driven by denaturants (temperature, surfactant).

Apart from tetravalent, we observe similar results for the trivalent ($AlCl_3$) salt exhibiting the validity of the observations for the multivalent salts, in general. The SANS data of the 5 wt. % BSA+80 mM $AlCl_3$ system with varying concentration of DTAB [Fig. 3(a)] show similar features as observed with Zr^{4+} ions, suggesting the coexistence of the free micelles and unfolded protein. Likewise, BSA does not form gel [inset of Fig. 3(b)] on increasing temperature in the presence of $AlCl_3$ and the scattering data [Fig. 3(b)] remain more or less the same (Table ST8 in Supplemental Material [26]), except for the rise in the scattering intensity in the low-Q region, indicating slight evolution of the attraction (aggregation) in the system. This suggests that trivalent ions are somewhat less effective than tetravalent ions in restricting the temperature-induced protein gelation. Consistent with this, no such behavior has been found in the case of divalent salt (e.g., $MgCl_2$). BSA in the presence of $MgCl_2$ follows the standard colloidal theory and does not show any reentrant behavior (Fig. S2 in Supplemental Material [26]) [12]. However, it has been reported that the physical state of the gels of denatured filamentous BSA formed by thermal denaturation followed by divalent ($CaCl_2$) salt-induced aggregation differs in their physical appearance with increasing $CaCl_2$ concentrations [42]. The transparent filamentous gels form at low and high $CaCl_2$ concentrations whereas at intermediate $CaCl_2$ concentrations turbid gels were obtained [42]. This suggests that divalent ions are also capable of tuning the gelation but are not able to prevent it. Moreover, the behavior has also not been seen even in the low concentration regime of the tri-(tetra)valent ions (i.e., before two-phase formation in Fig. S2 in Supplemental Material [26]), suggesting that strong condensation of the ions is required to obtain such unusual stability.

To conclude, we have shown the unusual stability of the protein against the usual denaturants (temperature and surfactant). The multivalent ions are believed to condense on the BSA proteins and tune the double layer around the molecule, which in turn prevent the denaturants to cause protein unfolding. The observed stability may not sustain in the cases where the denaturation is caused by means (e.g., urea, pressure), which in general do not substantially involve electrostatic interactions (Fig. S18 in Supplemental Material [26]). It will further be interesting to probe the effect of the different coions, as it is known that the different coions also alter the protein reentrant phase behavior [43].

[1] M. L. Hughes and L. Dougan, The physics of pulling polyproteins: A review of single molecule force spectroscopy using the AFM to study protein unfolding, Rep. Prog. Phys. **79**, 076601 (2016).

[2] L. Konermann, *Protein Unfolding and Denaturants* (John Wiley & Sons, Ltd., Chichester, 2012).

[3] F. Mallamace, C. Corsaro, D. Mallamace, S. Vasi, C. Vasi, P. Baglioni, S. V. Buldyrev, S.-H. Chen, and H. E. Stanley, Energy landscape in protein folding and unfolding, Proc. Natl. Acad. Sci. USA **113**, 3159 (2016).

[4] L. R. Khoury and I. Popa, Chemical unfolding of protein domains induces shape change in programmed protein hydrogels, Nat. Commun. **10**, 5439 (2019).

[5] D. Winogradoff, S. John, and A. Aksimentiev, Protein unfolding by SDS: The microscopic mechanisms and the properties of the SDS-protein assembly, Nanoscale **12**, 5422 (2020).

[6] J. N. Pedersen, J. Lyngsø, T. Zinn, D. E. Otzen, and J. S. Pedersen, A complete picture of protein unfolding and refolding in surfactants, Chem. Sci. **11**, 699 (2020).
[7] C. L. Dias, Unifying Microscopic Mechanism for Pressure and Cold Denaturations of Proteins, Phys. Rev. Lett. **109**, 048104 (2012).
[8] P. J. Rossky, Protein denaturation by urea: Slash and bond, Proc. Natl. Acad. Sci. USA **105**, 16825 (2008).
[9] S. Mehan, V. K. Aswal, and J. Kohlbrecher, Tuning of protein-surfactant interaction to modify the resultant structure, Phys. Rev. E **92**, 032713 (2015).
[10] A. Schön, B. R. Clarkson, M. Jaime, and E. Freire, Temperature stability of proteins: Analysis of irreversible denaturation using isothermal calorimetry, Proteins **85**, 2009 (2017).
[11] H.-X. Zhou and X. Pang, Electrostatic interactions in protein structure, folding, binding, and condensation, Chem. Rev. **118**, 1691 (2018).
[12] S. Kumar, I. Yadav, D. Ray, D. Saha, S. Abbas, V. K. Aswal, and J. Kohlbrecher, Evolution of interactions in the protein solution as induced by mono and multivalent ions, Biomacromolecules **20**, 2123 (2019).
[13] P. S. Sarangapani, S. D. Hudson, R. L. Jones, J. F. Douglas, and J. A. Pathak, Critical examination of the colloidal particle model of globular proteins, Biophys. J. **108**, 724 (2015).
[14] S. H. Behrens, D. I. Christl, R. Emmerzael, P. Schurtenberger, and M. Borkovec, Charging and aggregation properties of carboxyl latex particles: Experiments versus DLVO theory, Langmuir **16**, 2566 (2000).
[15] S. H. Behrens, M. Borkovec, and P. Schurtenberger, Aggregation in charge-stabilized colloidal suspensions revisited, Langmuir **14**, 1951 (1998).
[16] A. Stradner and P. Schurtenberger, Potential and limits of a colloid approach to protein solutions, Soft Matter **16**, 307 (2020).
[17] M. Boström, D. R. M. Williams, and B. W. Ninham, Specific Ion Effects: Why DLVO Theory Fails for Biology and Colloid Systems, Phys. Rev. Lett. **87**, 168103 (2001).
[18] F. Zhang, M. W. A. Skoda, R. M. J. Jacobs, S. Zorn, R. A. Martin, C. M. Martin, G. F. Clark, S. Weggler, A. Hildebrandt, O. Kohlbacher, and F. Schreiber, Reentrant Condensation of Proteins in Solution Induced by Multivalent Counterions, Phys. Rev. Lett. **101**, 148101 (2008).
[19] C. Pasquier, M. Vazdar, J. Forsman, P. Jungwirth, and M. Lund, Anomalous protein-protein interactions in multivalent salt solution, J. Phys. Chem. B **121**, 3000 (2017).
[20] O. Matsarskaia, F. Roosen-Runge, and F. Schreiber, Multivalent ions and biomolecules: Attempting a comprehensive perspective, ChemPhysChem **21**, 1742 (2020).
[21] S. Kumar, D. Ray, S. Abbas, D. Saha, V. K. Aswal, and J. Kohlbrecher, Reentrant phase behavior of nanoparticle solutions probed by small-angle scattering, Curr. Opin. Colloid Interface Sci. **42**, 17 (2019).
[22] A. Kubíčková, T. Křížek, P. Coufal, M. Vazdar, E. Wernersson, J. Heyda, and P. Jungwirth, Overcharging in Biological Systems: Reversal of Electrophoretic Mobility of Aqueous Polyaspartate by Multivalent Cations, Phys. Rev. Lett. **108**, 186101 (2012).
[23] L. Valencia, E. M. Nomena, S. Monti, W. R. Arbelaez, A. P. Mathew, S. Kumar, and K. P. Velikov, Multivalent ion-induced re-entrant transition of carboxylated cellulose nanofibrils and its influence on nanomaterials' properties, Nanoscale **12**, 15652 (2020).
[24] S. Kumar, D. Saha, S. Takata, V. K. Aswal, and H. Seto, Modifications in the nanoparticle-protein interactions for tuning the protein adsorption and controlling the stability of complexes, Appl. Phys. Lett. **118**, 153701 (2021).
[25] S. Kumar, I. Yadav, S. Abbas, V. K. Aswal, and J. Kohlbrecher, Interactions in reentrant phase behavior of a charged nanoparticle solution by multivalent ions, Phys. Rev. E **96**, 060602(R) (2017).
[26] See Supplemental Material at http://link.aps.org/supplemental/10.1103/PhysRevE.104.L012603 for details of experiments, data analysis, and additional data.
[27] F. Roosen-Runge, B. S. Heck, F. Zhang, O. Kohlbacher, and F. Schreiber, Interplay of pH and binding of multivalent metal ions: Charge inversion and reentrant condensation in protein solutions, J. Phys. Chem. B **117**, 5777 (2013).
[28] S. H. Arabi, B. Aghelnejad, C. Schwieger, A. Meister, A. Kerth, and D. Hinderberger, Serum albumin hydrogels in broad pH and temperature ranges: Characterization of their self-assembled structures and nanoscopic and macroscopic properties, Biomater. Sci. **6**, 478 (2018).
[29] O. Matsarskaia, L. Bühl, C. Beck, M. Grimaldo, R. Schweins, F. Zhang, T. Seydel, F. Schreiber, and F. Roosen-Runge, Evolution of the structure and dynamics of bovine serum albumin induced by thermal denaturation, Phys. Chem. Chem. Phys. **22**, 18507 (2020).
[30] K. Baler, R. Michael, I. Szleifer, and G. A. Ameer, Albumin hydrogels formed by electrostatically triggered self-assembly and their drug delivery capability, Biomacromolecules **15**, 3625 (2014).
[31] D. I. Svergun and M. H. J. Koch, Small-angle scattering studies of biological macromolecules in solution, Rep. Prog. Phys. **66**, 1735 (2003).
[32] K. Julius, J. Weine, M. Berghaus, N. König, M. Gao, J. Latarius, M. Paulus, M. A. Schroer, M. Tolan, and R. Winter, Water-Mediated Protein-Protein Interactions at High Pressures Are Controlled by a Deep-Sea Osmolyte, Phys. Rev. Lett. **121**, 038101 (2018).
[33] M. C. Abramo, C. Caccamo, D. Costa, G. Pellicane, R. Ruberto, and U. Wanderlingh, Effective interactions in lysozyme aqueous solutions: A small-angle neutron scattering and computer simulation study, J. Chem. Phys. **136**, 035103 (2012).
[34] Y. Liu, E. Fratini, P. Baglioni, W.-R. Chen, and S.-H. Chen, Effective Long-Range Attraction Between Protein Molecules in Solutions Studied by Small Angle Neutron Scattering, Phys. Rev. Lett. **95**, 118102 (2005).
[35] S. Kumar, V. K. Aswal, and J. Kohlbrecher, Small-angle neutron scattering study of interplay of attractive and repulsive interactions in nanoparticle-polymer system, Langmuir **32**, 1450 (2016).
[36] L. R. S. Barbosa, M. G. Ortore, F. Spinozzi, P. Mariani, S. Bernstorff, and R. Itri, The importance of protein-protein interactions on the pH-induced conformational changes of bovine serum albumin: A small-angle X-ray scattering study, Biophys. J. **98**, 147 (2010).
[37] T. T. Nguyen, A. Y. Grosberg, and B. I. Shklovskii, Macroions in Salty Water with Multivalent Ions: Giant Inversion of Charge, Phys. Rev. Lett. **85**, 1568 (2000).

[38] C. M. Jeffries, M. A. Graewert, C. E. Blanchet, D. B. Langley, A. E. Whitten, and D. I. Svergun, Preparing monodisperse macromolecular samples for successful biological small-angle X-ray and neutron scattering experiments, Nat. Protoc. **11**, 2122 (2016).

[39] D. Molodenskiy, E. Shirshin, T. Tikhonova, A. Gruzinov, G. Peters, and F. Spinozzi, Thermally induced conformational changes and protein–protein interactions of bovine serum albumin in aqueous solution under different pH and ionic strengths as revealed by SAXS measurements, Phys. Chem. Chem. Phys. **19**, 17143 (2017).

[40] W. Burchard and K. Kajiwara, The statistics of stiff chain molecules. I. The particle scattering factor, Proc. R. Soc. London, Ser. A **316**, 185 (1970).

[41] D. Saha, D. Ray, J. Kohlbrecher, and V. K. Aswal, Unfolding and refolding of protein by a combination of ionic and nonionic surfactants, ACS Omega **3**, 8260 (2018).

[42] H. Wu, P. Arosio, O. G. Podolskaya, D. Wei, and M. Morbidelli, Stability and gelation behavior of bovine serum albumin pre-aggregates in the presence of calcium chloride, Phys. Chem. Chem. Phys. **14**, 4906 (2012).

[43] M. K. Braun, A. Sauter, O. Matsarskaia, M. Wolf, F. Roosen-Runge, M. Sztucki, R. Roth, F. Zhang, and F. Schreiber, Reentrant phase behavior in protein solutions induced by multivalent salts: Strong effect of anions Cl^- versus $NO3^-$, J. Phys. Chem. B **122**, 11978 (2018).